J. Basic. Appl. Sci. Res., 2(9)9508-9516, 2012

ISSN 2090-4304
Journal of Basic and Applied Scientific Research
www.textroad.com

Numerical Study of Downward Co-Current Bubbly Flows

Mahmood Reza Rahimi, Soleiman Mosleh

Chemical Engineering Department, Yasouj University, Yasouj, 75918-74831, Iran

ABSTRACT

Downward turbulent bubbly flow in pipes was numerically studied. A bubble population balance model (BPBM) has been incorporated into computational fluid dynamics (CFD) and drag force, lift force, wall lubrication force and turbulence dispersion forces are considered into account. Flow parameters for liquid single phase and two-phase air-water bubbly flow in a 57.15 mm diameter and 3.06 m length vertical pipe were predicted. CFD-BPBM model predictions are in good agreement with experimental data.
KEY WORDS: CFD, Bubbly flow, Population balance modeling, Gas volume fraction, Liquid velocity, Downward flow.

1. INTRODUCTION

Turbulent gas–liquid bubbly flows are extensively used in various industrial applications. Downward flow can be encountered in industrial applications, for example in chemical reactors, through the drill string, and in the nuclear reactors under transient and accidental conditions.

In the gas-liquid two-phase flows, usually the ratio of the liquid phase density to the gas phase density is large. Therefore, this suggests that the downward flow can have rather different flow structure characteristics in comparison to the upward flow. Hence, the gravity effect should be considered in analysis.

Horizontal and upward two-phase flows were studied most broadly in publications [1-11]. CFD modeling of two-phase flows were focused recently in publications [6-8].

During the last decade, considerable interest was given to the study of downward bubbly flows, a review of such efforts can be find in recent papers of Terekhov and Pakhomov [12], Kashinsky et al, [13] and Sun et al. [14]. Numerical studies on the simulation of dynamics of downward flows was reported by Zaichik et al. [15] using diffusion-inertia approach. Lu and Trygvasson [16] used the method of direct numerical simulation (DNS) for investigating downward bubbly flow in a plane channel.

It can be said that in spite of the relatively large number of experimental studies in this field, the numerical studies of the hydrodynamics of downward two-phase flow were reported insufficiently. The main aim of this work is to examine the ability of proposed CFD model coupled with bubble population balance modeling (BPBM), especially for showing phase distribution, turbulent structure and liquid phase velocity, which are especially important from the stand point of engineering applications. In this study turbulent bubbly air-water two-phase flows in a circular pipe were investigated. The internal phase distribution of air-water bubbly flow in a 57.15 mm diameter 3.06 m length vertical downward pipe has been modeled using the 3-D Eulerian-Eulerian multiphase flow approach combined with bubble population balance modeling (BPBM). Important flow quantities such as local volume fraction, liquid velocity and the turbulent fluctuations were calculated and compared against experimental data of Wang et al. [9].

2. MODELING

Bubble size distribution (BSD) plays an important role in the phase structure, interphase forces, and hydrodynamic behaviours of two-phase gas-liquid flows. Therefore, spatial distribution of volume fraction and velocities of both phases are influenced by BSD. These influences can be taken into account in computational fluid dynamics (CFD) simulations. The population balance model provides an appropriate mathematical framework as an effective technique for the modeling of BSD.

The governing equations without interface heat and mass transfer, in the Eulerian–Eulerian frame, can be written as follows. The liquid phase was considered as the continuous and the gas phase as the dispersed phase. The dispersed phase is considered as discrete bubble sizes were tracked by solving an additional set of transport equations. These equations were progressively coupled with the flow equations during the simulations.

Continuity equation (liquid phase):

***Corresponding Author**: Soleiman Mosleh, Chemical Engineering Department, Yasouj University, mosleh_pa@yahoo.com, Telfax: +98-741-2221711

$$\frac{\partial}{\partial t}(\rho_l \alpha_l) + \nabla.(\rho_l \alpha_l \mathrm{u}_l) = 0 \quad (1)$$

Continuity equation (gas phase):

$$\frac{\partial}{\partial \mathrm{t}}(\rho_g \alpha_g \mathrm{f}_i) + \nabla.(\rho_g \alpha_g \mathbf{u}_g \mathrm{f}_i) = \mathrm{S}_i \quad (2)$$

and

$$S_i = P_i^B + P_i^C - D_i^B - D_i^C \quad (3)$$

The variable α represents volume fraction and the sum of each phasic volume fraction is equal to unity, f_i is the volume fraction of bubbles of group i (i=1-N) and Si is a source term that is algebraic sum of the death and birth of bubbles caused by coalescence and break-up processes. And P^B, P^C, D^B and D^C are respectively, the 'birth (or production)' and 'death (or consumption)' due to break-up and coalescence of bubbles. The production rates due to coalescence and break-up of bubbles were represented as:

$$P_i^C = \frac{1}{2}\sum_{k=1}^{N}\sum_{l=1}^{n} \chi_{i,kl} n_i n_j \quad (4a)$$

$$P_i^B = \sum_{j=1}^{n} \Omega(V_j : V_i) n_j \quad (4b)$$

And the death rate due to coalescence and break-up of bubbles are:

$$D_i^C = \sum_{j=1}^{n} \chi_{ij} n_i n_j \quad (4c)$$

$$D_i^B = \Omega_i n_i \quad (4d)$$

The relation between the bubble number density ni and gas volume fraction α_g is given by:

$$\alpha_g \mathrm{f}_i = \mathrm{n}_i \mathrm{V}_i \quad (5)$$

where V_i is the volume of a bubble of group i.

The break-up of bubbles in turbulent dispersions is represented by the model developed by Luo and sevendsen [17] and the coalescence rate taking into account turbulent collision by Prince and Blanch model [18].

The momentum conservation (for liquid phase):

$$\frac{\partial}{\partial t}(\rho_l \alpha_l \mathrm{u}_l) + \nabla.(\rho_l \alpha_l \mathrm{u}_l \mathrm{u}_l) = -\alpha_l \nabla p + \rho_l \alpha_l g - \nabla(\tau_l \alpha_l) + \mathrm{F}_{\mathrm{lg}} \quad (6)$$

The momentum conservation (for gas phase):

$$\frac{\partial}{\partial t}(\rho_g \alpha_g \mathrm{u}_g) + \nabla.(\rho_g \alpha_g \mathrm{u}_g \mathrm{u}_g) = -\alpha_g \nabla p + \rho_g \alpha_g g - \nabla(\tau_g \alpha_g) + \mathrm{F}_{gl} \quad (7)$$

Where u is the volume averaged velocity vector, p is the pressure, g is the gravity, τ is the phase shear stress tensor and $\mathrm{F}_{\mathrm{lg}} = -F_{gl}$ is the interphase force term. The terms on the right hand side of Eq's. (6 & 7) represent, from left to right, the pressure gradient, gravity, the viscous stress term and interphase momentum forces. Here P is assumed as the average pressure of the mixture phase. The total interphase force acting on the interfaces of two phases is the sum of several independent physical effects: effective stress, interfacial momentum exchange (drag and virtual mass forces), and the gravitational force. A recent paper by Lucas et al, [19] is covered the subject of non-drag forces modeling. The closure models for interfacial momentum exchange and turbulence effects are discussed next.

$$F_{lg} = F_D + F_L + F_{VM} + F_{WL} + F_{TD} \quad (8)$$

These forces represent the interphase drag force, lift force, virtual (added) mass force, wall lubrication force, and turbulence dispersion force, respectively. In this model the drag force, lift force, wall lubrication force and turbulence dispersion forces are considered into account. In the present model we have considered interfacial drag force that can be expressed as follows:

$$F_D = \frac{3}{4} C_D \alpha_g \rho_l \frac{1}{d_b} |u_l - u_g| (u_l - u_g) \quad (9)$$

The drag model of Ishii-Zuber [20] was used for the drag coefficient C_D. The lift force considers the interaction of the bubble with the shear field of the liquid. It acts perpendicular to the main flow direction and is proportional to the gradient of the liquid velocity field. A good review of lift force modeling is reported by Hibiki and Ishii [21], Here, it can be modeled as:

$$F_L^l = -F_L^g = C_L \alpha_g \rho_l (u_l - u_g) \times \nabla \times u_l \quad (10)$$

Where C_L is the lift coefficient and the superscripts l and g stands for the continuous (liquid) and dispersed (gas) phases. Where C_L is the lift coefficient determined using Tomiyama model [22], which is Eötvos number dependent:

$$C_L = \begin{cases} \min[0.2888 \tanh(0.121 \mathrm{Re}), f(Eo_g)] & EO_g < 4 \\ f(Eo_g) & 4 \le EO_g \le 10 \\ -0.27 & EO_g > 10 \end{cases} \quad (11)$$

Where the Eötvos number function is defined as:

$$f(Eo_g) = 0.00105 Eo_g^3 - 0.0159 Eo_g^2 - 0.0204 Eo_g + 0.474 \quad (12)$$

Here Re is the local Reynolds number of the gas phase (bubbles) and Eo_g is the modified Eötvos number of the gas phase:

$$Eo_g = \frac{g(\rho_l - \rho_g) d_H^2}{\sigma} \quad (13)$$

Where dH is the maximum horizontal bubble dimension that is calculated using empirical correlation of Wellek et al.[23]

$$d_H = d_b (1 + 0.163 Eo^{0.757})^{1/3} \quad (14)$$

And db is Sauter mean diameter of bubbles, and Eötvos number is:

$$Eo = \frac{g(\rho_l - \rho_g) d_b^2}{\sigma} \quad (15)$$

The turbulent dispersion force can be modeled as:

$$F_{TD}^l = -F_{TD}^g = -C_T \rho_l k_l \nabla \alpha_l \quad (16)$$

Where k_l is the liquid turbulent kinetic energy per unit mass. Liquid flow rate between bubble and the wall is lower than between the bubble and the outer flow, and this is the origin of the wall lubrication force. This results in a hydrodynamics pressure difference driving bubble away from the wall. This force is expressed as:

$$F_{WL}^l = -F_{WL}^g = -\alpha_g \rho_l \frac{u_r - (u_r n_w) n_w)^2}{d_b} \max[C_1 + C_2 \frac{d_b}{y_W}, 0] n_W \quad (17)$$

here, $u_r = u_l - u_g$ is the relative velocity between phases, d_b is the disperse phase mean diameter, y_w is the distance to the nearest wall, and n_w is the unit normal (away from the wall). The model constants C_1=-0.0064 and C_2=0.016 where proposed by Krepper et al. [24]. The force is set to zero if the wall

distance satisfies the following condition: $y_w > (C_{w2}/C_{w1})d_b$ .The local Sauter mean diameter of bubbles in eq. (17) is defined as:

$$d_b = \frac{1}{\sum f_i / d_i} \tag{18}$$

Turbulence is taken into consideration for the continuous phase using k- ε model and the influence of the dispersed phase on the turbulence of the continuous phase is taken into account with the Sato's bubble-induced turbulent viscosity model [10]. The governing equations for the turbulent kinetic energy k and turbulent dissipation ε are:

$$\frac{\partial}{\partial t}(\rho_l \alpha_l k) + \frac{\partial}{\partial x_i}.(\rho_l \alpha_l u_l k) = \frac{\partial}{\partial x_i}(\alpha_l(\mu_l + \frac{\mu_{l,tur}}{\sigma_k})\frac{\partial k}{\partial x_i} + \alpha_l(G - \alpha_l \rho_l \varepsilon_l)$$

$$\frac{\partial}{\partial t}(\rho_l \alpha_l \varepsilon_l) + \frac{\partial}{\partial x_i}.(\rho_l \alpha_l u_l \varepsilon_l) = \frac{\partial}{\partial x_i}(\alpha_l(\mu_l + \frac{\mu_{l,tur}}{\sigma_\varepsilon})\frac{\partial \varepsilon_l}{\partial x_i}) + \alpha_l \frac{\varepsilon_l}{k}(C_{\varepsilon 1} G - C_{\varepsilon 2} \alpha_l \rho_l \varepsilon_l) \tag{14}$$

$$\mu_{l,tur} = C_\mu \rho_c \frac{k_c^2}{\varepsilon_c}$$

Where $C_{\varepsilon 1}$, $C_{\varepsilon 2}$, C_μ , σ_k , σ_ε are the standard $k-\varepsilon$ model constants and G is the turbulence production term. Using the standard $k-\varepsilon$ model combined with Sato's bubble-induced turbulent viscosity model [10] the turbulent viscosity of the continuous phase is calculated by

$$\mu_{\alpha,eff} = \mu_{\alpha,lam} + \frac{\mu_{\alpha,tur}}{\sigma_k} + \mu_S \tag{15}$$

Where μ_S is Sato's bubble-induced turbulent viscosity, no turbulence model was used for gas (dispersed) phase.

2. SOLUTION METHOD

A 3-D CFD model for downward flow in a vertical pipe was combined with bubble population balance modeling (BPBM). Governing conservation equations are discretised using finite volume method, upwind scheme was used for all equations, SIMPLEC algorithm was used for pressure-velocity coupling. Liquid (Water) was considered as the continuous phase, and gas (air) as the dispersed phase. The BPBM model was used to modeling the non-uniform bubble size distribution and bubbles are equally divided into five groups. The mathematical model was applied in the CFD commercial code for numerical studies, with the construction of a particular numerical grid and with its own subroutine in FORTRAN language for the closure equations of model.

Uniform gas and liquid velocities and average volume fractions have been specified in the pipe inlet as boundary condition. Zero relative average static pressure was used as the pipe outlet boundary condition. No slip boundary conditions were used at wall. For initiating the numerical solution average volume fraction and uniform liquid velocity profile are specified. Grid independency study was done using several grids and several simulations were done applying gradually larger number of grid points starting from about 80000, there was seen practically no change in the gas volume fraction and liquid velocity profiles when the grid number increased beyond 580000.

An air-water loop was used by Wang et al. [9] had a 57.15 mm diameter and 3.06 m length test section for measurements of both up and down flows. A single sensor cylindrical hot-film probe was used to measure the mean and fluctuations in the axial liquid velocity and the local volume fraction. Reynolds stress components in the liquid phase, measured using a special 3-D conical probe. A typical grid structure is shown in Fig. 1.

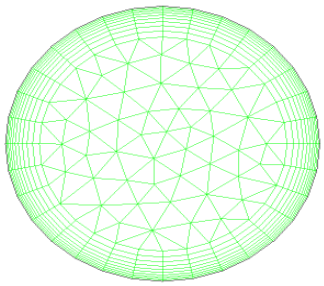

Figure1. Grid structure.

The first layer in inflated layer near the wall was set at a distance from the wall to take a value of the y+ in the range from 30 to 40, in order to achieve stable solutions avoiding numerical oscillations and also to have a precise wall lubrication force modeling.

3. RESULTS AND DISCUSSION

The proposed CFD-BPBM model was tested by using this model for an air/water flow system used by Wang et al. [9] had a 57.15 mm internal diameter. At first, the CFD model was tested for single liquid phase flow of water in the same system. As can be seen in Fig. 2, the axial component of liquid velocity is compared against experimental data [9]. The results are consistent and CFD model results are within 4.6% of experimental ones. The predicted values of air volume fraction were presented in Figs 3-5.

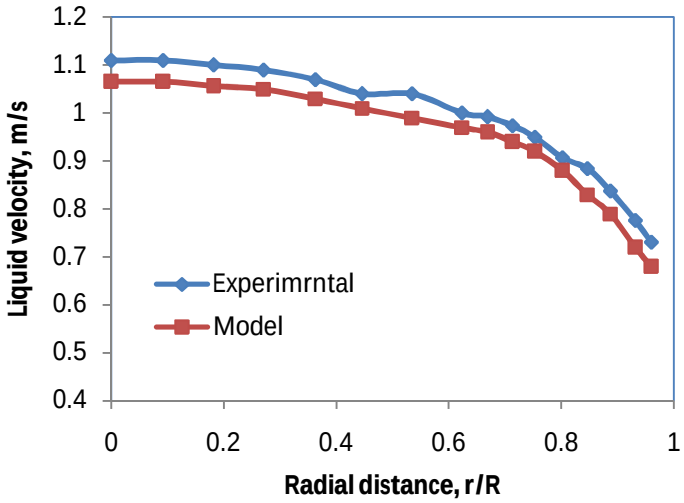

Fiqure 2. Axial liquid velocity distributions in comparison to experimental data [9], z/D = 35, Re_L=44000

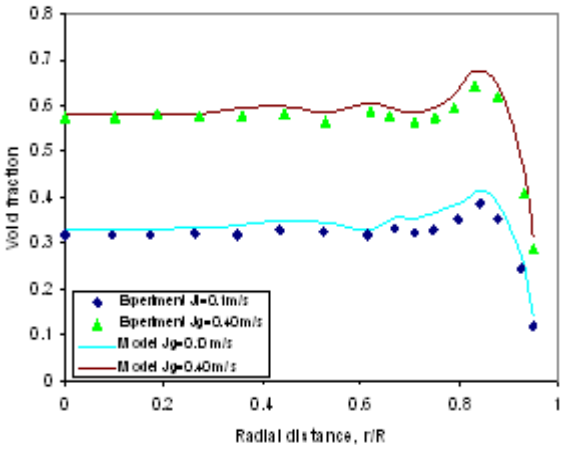

Figure 3. Air volume fraction, J_L=0.94 m/s, in comparison to experimental data [9].

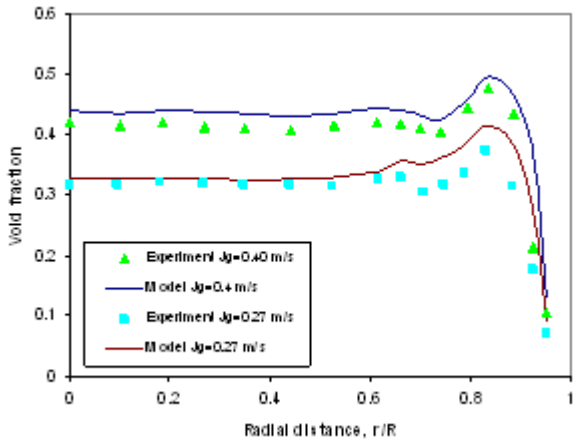

Figure 4. Air volume fraction, J_L=0.71 m/s, in comparison to experimental data [9].

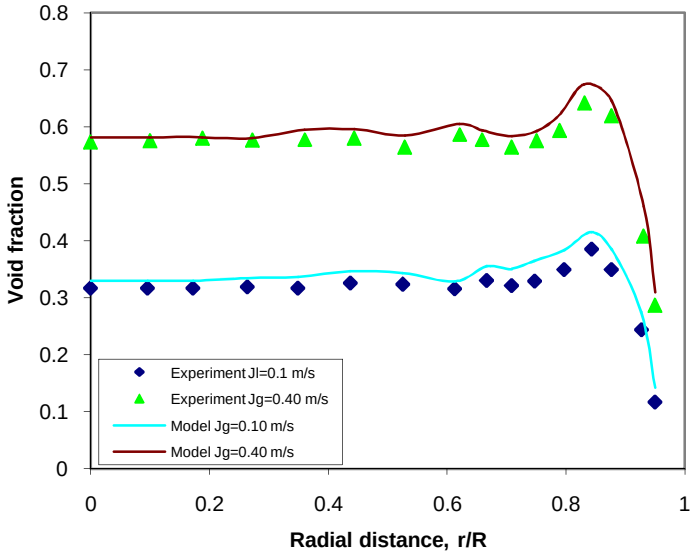

Figure 5. Air volume fraction, J_L=0.40 m/s, in comparison to experimental data [9].

From the phenomenological view point, the phase distribution patterns along the radial direction exhibits three basic types of distributions: “core-peaked”, “bell-typed”, and “off-center”, as categorized by Hibiki et al [4] for downward two-phase flows.

Figs. 3-5 show the volume fraction distributions obtained from the model comparing with the experimental data at the dimensionless axial position z/D = 35. The results are follows the correct trend, as can be seen in this figure. It was found that local volume fraction distribution was shown a maximum in the near-wall region, but in a distance away from the wall, and tend to zero at the wall with a sharp gradient in the near-wall region and a flat terrain in the core of the flow. So, the absence of bubbles in the near-wall region means that bubbles tended to migrate away from the wall; it was also shown the peaking and coring phenomena. Therefore, predictions are in good agreement with measurements within the error bands and peaking and coring of volume fraction are well-predicted.

Figs. 6 and 7 show the local radial liquid velocity distributions at z/D = 35 for liquid single phase flow and two phase flow with specified gas and liquid superficial velocities. The simulation results of liquid velocity profiles obtained from this modeling compared against measurements and a good agreement with experimental data was found. Relative to liquid single phase flow the presence of bubbles in two phase flow result in the formation of a plateau in the liquid velocity distribution, the liquid velocity distribution shows a maximum in the near-wall region and exhibit nearly flat in the core region. For single liquid phase

the maximum of liquid velocity is located in the core region, but is in the near wall region for two-phase flow, means a displacement out from the pipe axis and core region.

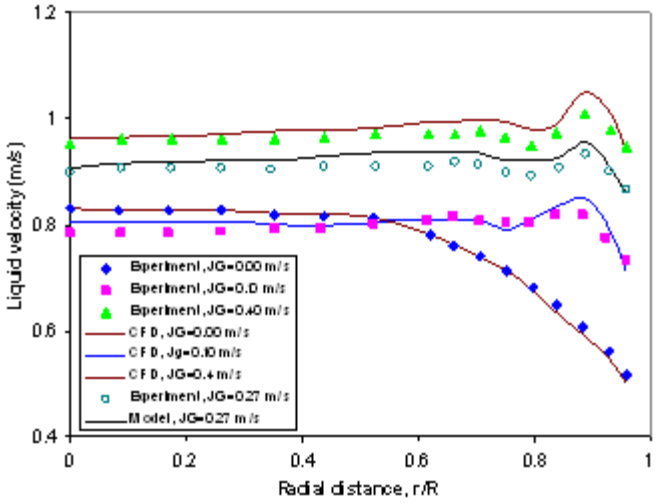

Fiqure 6. Local radial liquid velocity distributions in comparison with experimental data [9], z/D = 35 and J_L=0.71 m/s

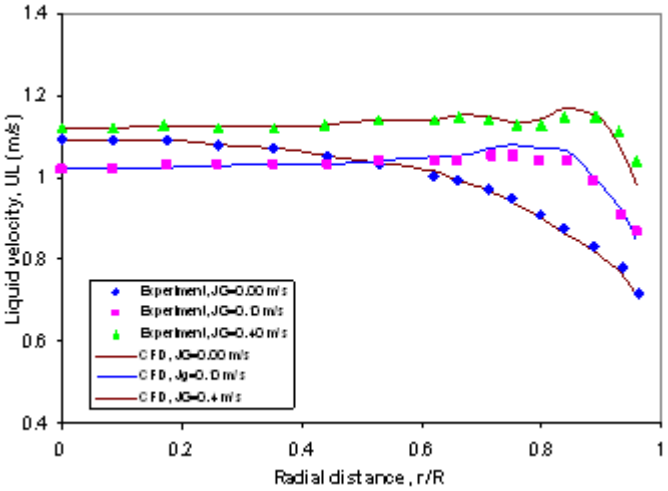

Fiqure 7. Local radial liquid velocity distributions in comparison with experimental data [9], z/D = 35 and J_L=0.94 m/s

In two-phase flows, the turbulent fluctuations showed nearly flat profiles in the core region (r/R < 0.6) and, except near the wall, the turbulence structure was more anisotropic compared to single-phase flows. Normally, the increase in liquid velocity augmented the level of turbulence in the near wall (r/R > 0.6) region.

In comparison to single liquid phase, the presence of bubbles in downward turbulent two-phase flow decreases the magnitude of liquid velocity fluctuations in the near-wall region and increases in the core region is significant, increases dissipation as well as enhancing the production of turbulence kinetic energy. For higher air flow rates the presence of bubbles suppressed the level of liquid velocity fluctuations. The maximum liquid velocity and the volume peak did not take place at the same location, probably because of the counteracting effect of high shear stress near the wall as shown by Wang et al, [9].

5. Conclusion

The behavior of air-water turbulent bubbly flow in a 57.15 mm internal diameter 3.06 m length vertical pipe has been modeled using the 3-D CFD model combined with bubble population balance modeling (BPBM). Important flow parameters such as local volume fraction and liquid velocity were calculated and compared against experimental data of Wang et al, [9]. This modeling was shown that volume fraction profile exhibited a maximum peak near the wall and the liquid velocity profile was flattened by the presence of the bubbles, in comparison to single liquid phase. In the core region (r/R< 0.6)

the volume fraction frequently showed nearly flat profiles. The results was certifies the capability of this combined CFD-BPBM model to capture the main phenomena occurred in downward two-phase flow in pipes.

6. REFRENCES

1. Karimi, H., Rahimi, M. R., 2008. A Robust Classification method for the Prediction of Two Phase Flow Pattern, using Ensemble Classifiers Technique, 11th Int. Conf. on Multiphase Flow in Industrial Plants, 443-451.

2. Kocamustafaogullari, G., M. Ishii, 1995. Foundation of the interfacial area transport equation and its closure relations. Int. J. Heat Mass Trans. 38: 481–493.

3. Wang, T., J. Wang, Y. Jin, 2005. Population Balance Model for Gas−Liquid Flows: Influence of Bubble Coalescence and Breakup Models, Ind. Eng. Chem. Res., 44: 19.

4. Hibiki, T., M. Ishii, Z. Xiao, 2001. Axial interfacial area transport of vertical bubble flows. Int. J. Heat Mass Trans. 44: 1869–1888.

5. Hibiki, T., M. Ishii, 2002. Development of one-group interfacial area transport equation in bubbly flow systems. Int. J. Heat Mass Trans. 45: 2351–2372.

6. Ekambara, K., R.S. Sanders, K. Nandakumar, J.H. Masliyah, 2008. CFD simulation of bubbly two-phase flow in horizontal pipes, Chemical Engineering Journal 144: 277–288.

7. Cheung, C.P., G.H.Yeoh, J.Y. Tu, 2007. On the modeling of population balance in isothermal vertical bubbly flows – Average bubble number density approach. Chem. Eng. Process. 46: 742–756.

8. Sarı, S., S. Ergün, M. Barık, C. Kocar, C. N. Sökmen, 2009. Modeling of isothermal bubbly flow with ınterfacial area transport equation and bubble number density approach. Annals of Nuclear Energy 36: 222-232.

9. Wang, S. K., S. J. Lee, O. C. Jones, R. T. Lahey, 1987. 3-D turbulece structure and phase distribution measurements in bubbly two-phase flows. Int. J. Multiphase flow, 13: 327-343.

10. Sato, Y. M. Sadatomi, K. Sekoguchi, 1981. Momentum and heat transfer in two-phase bubbly flow—I. International Journal of Multiphase Flow 7: 167–178.

11. Serizawa, A., I. Kataoka, 1988. Phase distribution in two-phase flow. In: Afgan, N.H. (Ed.), Transient Phenomena in Multiphase Flow. Washington, DC, pp. 179–224.

12. Terekhov, V. I., M. A. Pakhomov, 2008. The Effect of Bubbles on the Structure of Flow and the Friction in Downward Turbulent Gas–Liquid Flow. High Temperature 46: 854–860.

13. Kashinsky, O. N., P. D. Lobanov, M. A. Pakhomov, V. V. Randin, V. I. Terekhov, 2006. Experimental and numerical study of downward bubbly flow in a pipe. International Journal of Heat and Mass Transfer 49: 3717–3727.

14. Sun, X., S. Paranjape, S. Kim, B. Ozar, M. Ishii, 2004. Liquid velocity in upward and downward air–water flows. Annals of Nuclear Energy 31: 357–373.

15. Zaichik, L. I., A. P. Skibin, S. L. Soloviev, 2004. Simulation of the distribution of bubbles in a turbulent liquid using a diffusion-inertia model, High Temp. 42: 111–118.

16. Lu, J., G. Trygvasson, 2006. Numerical study of turbulent bubbly downflows in a vertical channel. Phys. Fluids A, 18: Paper 103302.

17. Luo, H., H. Svendsen, 1996. Theoretical model for drop and bubble break-up in turbulent dispersions. AIChE J. 42: 1225–1233.

18. Prince, M. J., H. W. Blanch, 1990. Bubble coalescence and break-up in air sparged bubble columns. AIChE J. 36: 1485–1499.

19. Lucas, D., E. Krepper, N. M. Prasser, 2007. Use of models for lift,wall and turbulent dispersion forces acting on bubbles for poly-disperse flows. Chem. Eng. Sci. 62: 4146 – 4157.

20. Ishii, M., N. Zuber, 1979. Drag coefficient and relative velocity in bubbly, droplet or particulate flows. AIChE J. 25: 843–855.

21. Hibiki, T., M. Ishii, 2007. Lift force in bubbly flow systems. Chem. Eng. Sci. 62: 6457 – 6474.

22. Tomiyama, A., 1998. Struggle with computational bubble dynamics, 3rd International Conference on Multiphase Flow, ICMF-2004, Lyon, France, June 8–12, pp 1–18.

23. Wellek, R. M., A. K. Agrawal, A. H. P. Skelland, 1966. Shapes of liquid drops moving in liquid media. AIChE J. 12: 854.

24. Krepper, E., D. Lucas, H. M. Prasser, 2005. On the modelling of bubbly flow in vertical pipes, Nuclear Engineering and Design 235: 597–611.